

Poly(ethylene oxide)/lithium triflate phase diagram

J.-F. Moulin, P. Damman, M. Dosière*

Laboratoire de Physico-Chimie des Polymères, Université de Mons-Hainaut 20, Place du Parc, B-7000 Mons, Belgium

Received 2 October 1998; received in revised form 3 November 1998; accepted 3 November 1998

Abstract

The complete phase diagram of the poly(ethylene oxide)/lithium trifluoromethane sulfonate polymer electrolyte was determined by combined X-ray diffraction and differential scanning calorimetry. The sample preparation has dramatic effects on morphology and consequently on the phase diagram. The existence of three different molecular adducts involving the polymer and the salt was deduced from the phase diagram. These adducts transform into each other by peritectic reactions. Moreover, two different forms of pure lithium trifluoromethane sulfonate were observed. This polymorphism was studied by X-ray diffraction and differential scanning calorimetry. It was demonstrated that this salt undergoes a transition to a phase of higher symmetry at 179°C. An orthorhombic unit cell ($a = 1.496$ nm, $b = 1.475$ nm, $c = 1.425$ nm) was proposed for the high temperature form of the salt. © 1999 Elsevier Science Ltd. All rights reserved.

Keywords: Polymer electrolytes; Phase diagram; Poly(ethylene oxide)

1. Introduction

Polymer electrolytes, composed of inorganic salts dissolved in a solid polymer (usually poly(ethylene oxide), or PEO) matrix have raised high interest since their discovery in the late 1970s [1]. These systems display relatively large ionic conductivities in the solid state and have actual applications e.g. as separators in thin film batteries. Beside this practical importance, the study of their structure and properties brings more fundamental insight on molecular interactions and complexation. The phase diagram of these polymer electrolytes gives essential information for characterization of properties or structural studies, i.e. not only the nature and amounts of each phase in presence for given composition and temperature, but also about the existence and type of transformations these phases may undergo. In most PEO/alkali salts a molecular adduct with a 3 monomers/1 cation stoichiometry ($3\text{EO}/1\text{M}^+$, salt molar composition $X_s = 0.25$) is observed. These compounds all have the same general crystal structure with the polymer chains wrapping around the cations in a (TTG TTG TT-G)₂ conformation [2–4]. In some cases the existence of $1\text{EO}/\text{M}^+$ and other adducts was reported [3]. The polymorphism in these systems illustrates the great conformational flexibility of PEO that allows it to maximize the interactions with the host molecules without too high

penalty in terms of intramolecular energy [5]. Although the PEO/lithium trifluoromethane sulfonate (LiTf, or triflate) system has been extensively described [6,7], several questions remained open concerning the high salt concentration side of the phase diagram and this prompted our study. Preliminary experiments [8] clearly illustrated the complex polymorphism and the complications arising from the behaviour of the pure salt. It was also soon realized that the sample preparation procedure was the key factor in such a study.

In the present paper the complete PEO/LiTf phase diagram obtained by combined time resolved X-ray diffraction experiments and differential scanning calorimetry is described. This diagram is used to identify the different phases, including the two new PEO/LiTf adducts, and their transitions.

2. Experimental

Low molecular weight PEO ($\langle M_w \rangle = 35\,000$) kindly provided by Hoechst and high molecular weight PEO ($\langle M_w \rangle = 5 \times 10^6$) purchased from Aldrich were used without further purification. The polymers as well as Lithium triflate (Sigma Aldrich) were dried overnight at 120°C under vacuum. Most polymer electrolyte samples were cast from solution but some were prepared by quenching from the melt. Anhydrous methanol (Aldrich 99 + %) kept on molecular sieve (4Å) was used to prepare salt and polymer solutions (concentration c.a. 10% w/v). Accurately weighed

* Corresponding author.

E-mail address: dosiere@umh.ac.be (M. Dosière)

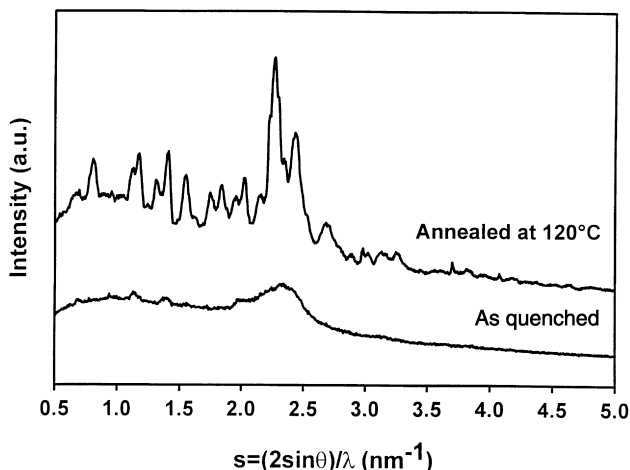


Fig. 1. X-ray diffraction pattern of PEO($M_w = 5 \times 10^6$)/LiTf polymer electrolyte illustrating the effect of annealing on crystallinity.

amounts of these salt and PEO solutions were mixed to obtain the different polymer electrolyte stoichiometries. The solutions were then cast on a PTFE foil kept at 50°C under a stream of dry air. After 30 minutes the samples were placed under vacuum at 50°C for 15 hours to ensure complete drying. The samples with $X_s < 0.25$ were then used without further treatment whereas the more concentrated samples were annealed for 15 hours at 110°C under vacuum. This procedure gave a crystalline powder that was kept in a dry box before use for calorimetric or X-ray experiments. Differential scanning calorimetry (DSC) measurements were made on a TA2920 calorimeter. The sample pans were filled with c.a. 5 mg of polymer electrolyte powder and sealed in a dry glove box. All thermograms were obtained at a heating rate of 10°C/min. Wide angle X-ray diffraction (WAXD) experiments were performed on the D43 synchrotron beamline at LURE using a modification of a Guinier–Lenne camera. The diagrams were recorded on an image plate (Molecular Dynamics) with

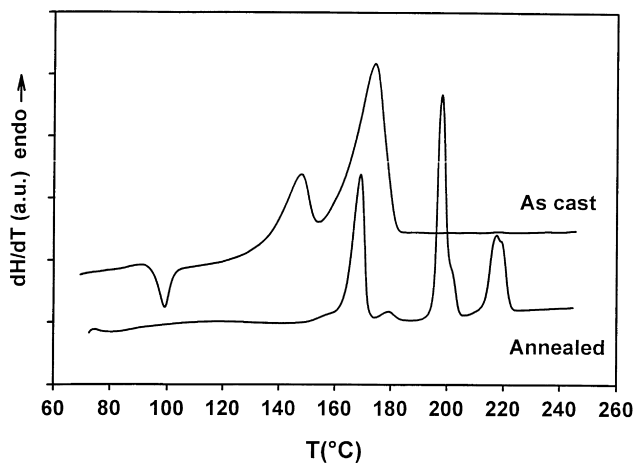


Fig. 2. Thermograms of a PEO($M_w = 35\,000$)/LiTf polymer electrolyte illustrating the effect of preparation procedure on the melting behaviour.

$88 \times 88 \mu\text{m}^2$ pixel size which was continuously translated behind a fixed 1mm wide slit. The entire evolution of the WAXD spectrum during heating could thus be recorded on a single image plate. The samples, prepared in a glove box, consisted of a small amount of polymer electrolyte powder placed between two KAPTON foils to protect it from moisture. They were heated using a Mettler FP82HT microscopy hot stage. The WAXD data were analyzed by deconvoluting the region of interest of the spectra using the Levenberg–Marquardt algorithm.

3. Results

3.1. Sample preparation

At the beginning of this study we focused our attention on the influence of the sample preparation procedure on morphology. The PEO/salt mixtures were first prepared by quenching from the melt because this technique allows an accurate and reproducible control of the thermal history of the system. Fig. 1 illustrates that the X-ray diffraction pattern obtained for a PEO ($M_w = 5 \times 10^6$)/LiTf mixture obtained by quenching from the melt consists of a broad amorphous halo with very faint diffraction peaks. It is quite clear that, because of the strong electrostatic interactions between PEO and inorganic salts that raise the glass transition temperature, quenching from the melt may lead to metastable amorphous systems [9]. Reproducible calorimetric results allowing phase diagram determination can thus only be obtained after suitable thermal treatment of the samples. Annealing the previous high molecular weight PEO/LiTf sample at 120°C for 12 hours gave a semi-crystalline film that displayed intense X-ray reflections (Fig. 1). This technique could unfortunately not be used for salt molar fractions higher than $X_s = 0.33$ because of the very high melting points in this region of the phase diagram. We then turned to solvent evaporation for the preparation of the polymer electrolyte. Incomplete crystallization of the samples was also observed and the as-cast PEO/LiTf mixtures remained largely amorphous for relatively long periods of time. The thermograms of such samples displayed pronounced exotherms around 100°C–120°C. Moreover, as the crystallinity slowly developed, thermograms of different samples taken from the same polymer electrolyte batch were not reproducible making the determination of a phase diagram impossible. To overcome this problem the polymer electrolyte samples were annealed as described in the experimental section to obtain highly crystalline powders. The influence of this thermal treatment upon phase behaviour of a sample having $X_s = 0.515$ is illustrated in Fig. 2. The as cast sample thermogram displays an exotherm and two broad endothermic transitions whereas, for the annealed sample these transitions are replaced by a series of much sharper endotherms.

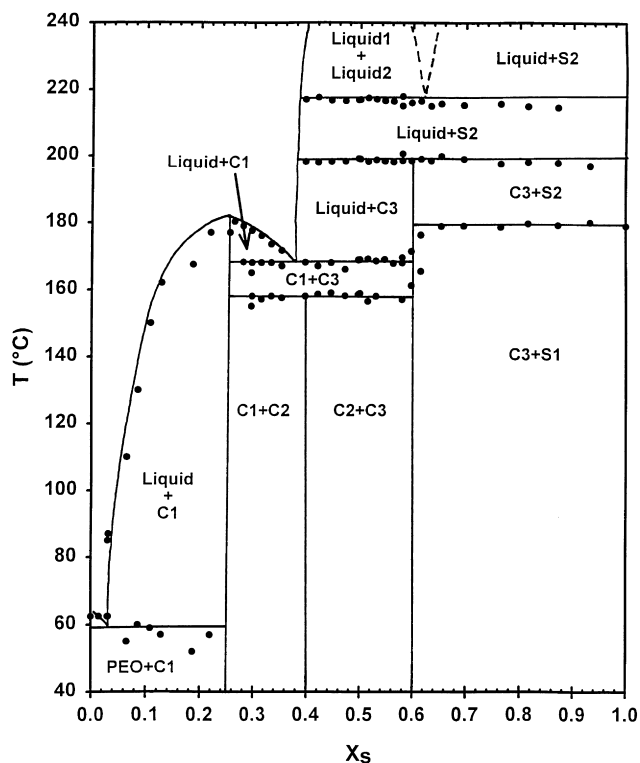


Fig. 3. PEO($M_w = 35\,000$)/LiTf phase diagram.

3.2. Calorimetric investigations

Once a satisfactory sample preparation method was established, the phase diagram was obtained from the DSC data (Fig. 3). Apart from the well known [6] low concentration side of this diagram where the usual eutectic behaviour and the congruently melting 3EO/1Li compound (hereafter referred to as C1) are observed, several transitions were detected. Most of these transitions appear at fixed temperature independently of composition. The transition lines at 158°C, 168°C and 179°C are interrupted around $X_s = 0.60$. The heat of reaction associated with each of the transitions is plotted against the molar composition in Fig. 4. The transition at 158°C, 168°C, 198°C and 218°C exhibit a Δh vs. X_s dependence that can be described by sets of two linear segments intersecting at the maximal Δh for each transition. The Δh of the transition at 179°C continuously increases from $X_s = 0.60$ to $X_s = 1$.

The assignment of the phase transitions is described below.

3.3. Wide angle X-ray diffraction

In order to identify the crystalline compounds involved in each transition, time resolved wide angle X-ray diffraction experiments were performed and the diffractograms of PEO/LiTf mixtures of various compositions recorded as a function of temperature.

The polymorphic transformation of the pure salt at high

temperature, has to our knowledge not been reported before. DSC indicated that LiTf undergoes a phase transition at 179°C and X-ray diffraction confirmed that this transition is a solid–solid modification. Fig. 5 gives the diffractograms of pure LiTf at room temperature and at 200°C respectively, the lower number of reflections indicates a higher symmetry for the high temperature polymorph. Time resolved X-ray measurements further confirmed that the 179°C transition is associated with this unit cell modification. The plot of the position and intensity of the first reflection as a function of temperature displays a clear break around 180°C (Fig. 6(a) and (b)); at this temperature, the (001) reflection at 0.946 nm^{-1} , which is characteristic of the monoclinic low temperature polymorph [10], vanishes while the 0.978 nm^{-1} reflection corresponding to the high temperature form develops. The orthorhombic unit cell parameters of the high temperature form of LiTf were determined by trial and error yielding: $a = 1.496\text{ nm}$, $b = 1.475\text{ nm}$, $c = 1.425\text{ nm}$ at 200°C. Table 1 gives the indexation of the different reflections for the high temperature form of LiTf.

During the X-ray diffraction study of different PEO/LiTf mixtures new reflections that could be attributed neither to the pure salt nor to the 3EO/1Li (C1) compound (Fig. 7) were observed. The evolution of the intensity of these reflections as a function of temperature is plotted in Figs. 8, 9 and 10 for three samples. Three distinct behaviours are observed. For $X_s = 0.334$ (Fig. 8) the 1.010 nm^{-1} reflection disappears around 155°C whereas the intensity of the 1.278 nm^{-1} reflection slightly increases before vanishing around 180°C, simultaneously with the 1.117 nm^{-1} peak. For higher salt content the intensity of the reflection around 1 nm^{-1} increases either continuously, as in the case of the $X_s = 0.515$ sample (Fig. 9), or passes through a maximum around $T = 190^\circ\text{C}$ for the $X_s = 0.654$ sample (Fig. 10). The position of this reflection (Fig. 11) shifts from 1.010 nm^{-1} (sample $X_s = 0.334$ at low temperature) to 0.965 nm^{-1} (samples $X_s = 0.515$ and $X_s = 0.654$ at high temperature). This change is not monotonous but rather shows breaks around 165°C and 180°C.

4. Discussion

The observed phase behaviour depends strongly on the sample preparation procedure. In the case of samples prepared from solutions the final structure results from an unknown pathway through a three components phase diagram (polymer–salt–solvent). In actual fact, dissolution of the polymer in a good solvent leads to a coil expansion which is, at least sterically, favourable to ion–polymer interactions. In contrast, if the polymer–salt interactions are less favourable than the polymer–solvent interactions, the eventual molecular compounds between PEO and salt should form only when most of the solvent has evaporated. This should lead to a much less organized structure than in the case where precomplexation occurs in solution.

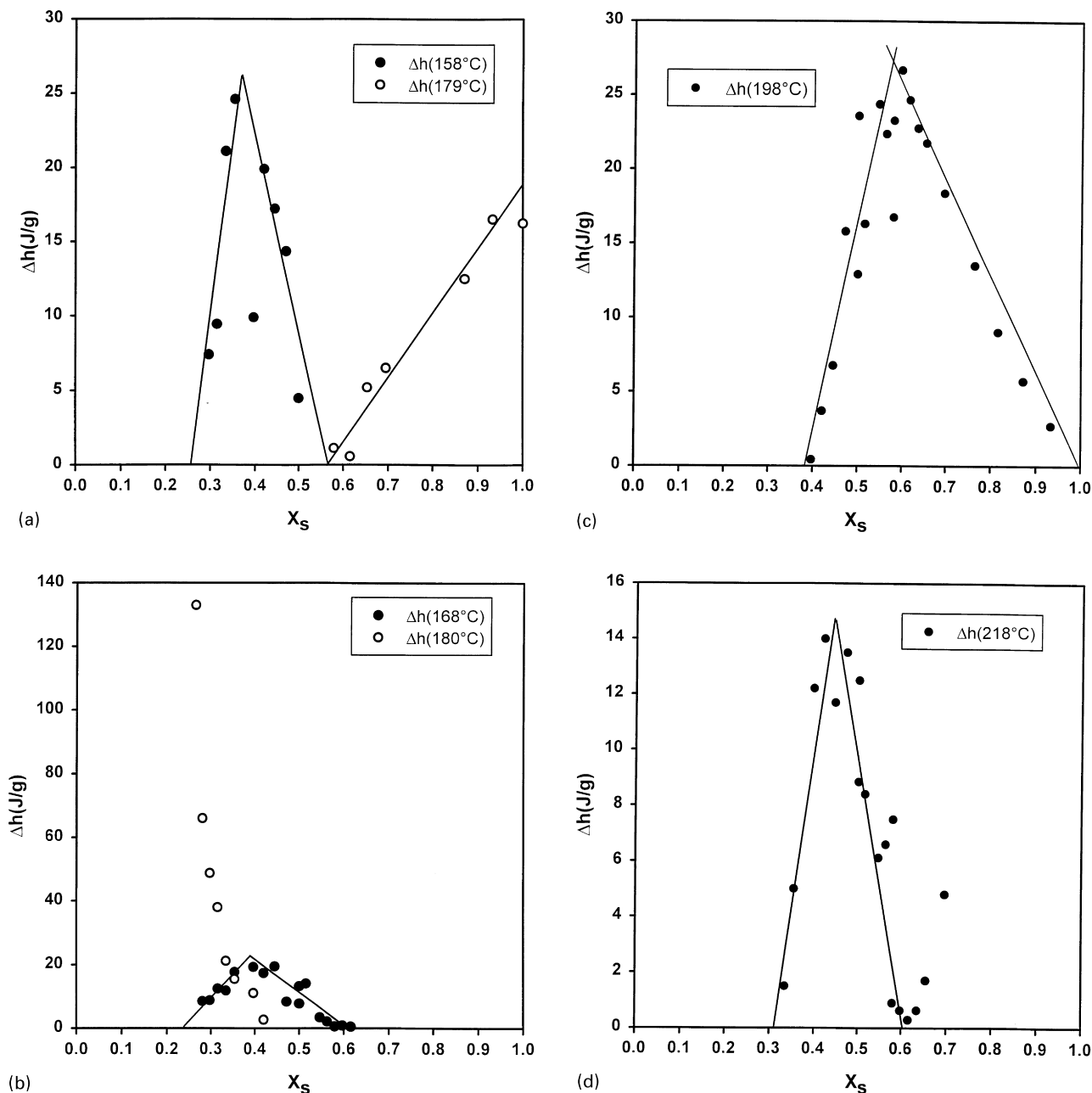


Fig. 4. (a) Heat of reaction associated with the 158°C and the 179° transitions; (b) Heat of reaction associated with the 168°C transition and the C1 congruent melting around 180°C; (c) Heat of reaction associated with the 198°C transition; (d) Heat of reaction associated with the 218°C transition.

Separation into pure solid salt and pure solid PEO can also occur even if, from the thermodynamic point of view, the molecular compounds are favoured. Different procedures can thus potentially lead to different final morphologies. For PEO/LiClO₄/Methanol systems, which should be quite similar to PEO/LiTf/Methanol, Banka et al. [11] have shown that salt precomplexation occurs in solution, and also established that the complexes are formed mainly in the outer portion of the coils. The latter observation suggests that some heterogeneity should still exist after solvent removal, and that a uniform distribution of the salt can only

be obtained after adequate thermal treatment of the sample.

We now analyse the results obtained for the PEO/LiTf samples prepared from solution. The large number of calorimetric transitions involving equilibrium between three phases (invariant transitions for a two components system) suggests the existence of several PEO/LiTf molecular compounds. It is clear, from the discontinuity of the lines at 158°C, 168°C and 179°C around $X_s = 0.60$ (Fig. 3), that this stoichiometry corresponds to one of the phase diagram boundary and that there lies one of the new molecular compounds (C3). For the 158°C transition, the Δh vs. salt

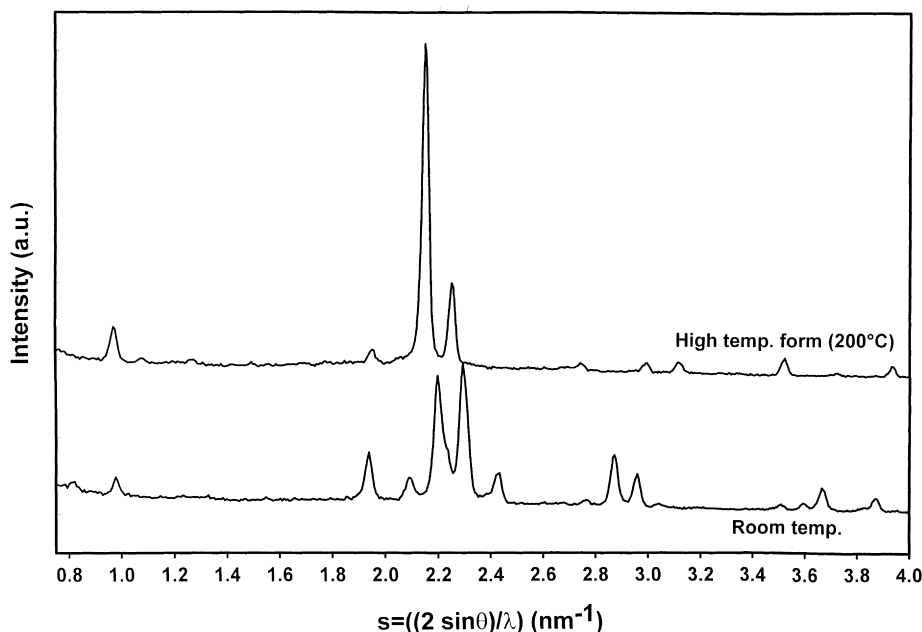


Fig. 5. X-ray diffractogram of pure LiTf at room temperature (lower curve) and at 200°C (upper curve).

mole fraction (X_s) evolution in Fig. 4(a) indicates that this reaction proceeds only in a composition range going from $X_s = 0.25$ (C1 compound) up to $X_s = 0.60$ (presumed C3 compound). X-ray diffraction data indicate (Fig. 8) that for a $X_s = 0.334$ sample this reaction is accompanied by the disappearance of the reflection near 1 nm^{-1} (1.010 nm^{-1} at 140°C , see Fig. 11) while the reflection at 1.278 nm^{-1} develops and the C1 reflection (at 1.117 nm^{-1}) remains almost unaffected. The reflection at 1.010 nm^{-1} should thus be attributed to a new crystalline phase C2, having a $X_s = 0.60$ for which the Δh (158°C) measured by DSC is the largest whereas the reflection at 1.278 nm^{-1} is characteristic of the C3 compound. This also shows that the 158°C reaction corresponds to the decomposition of the C2 phase into the C1 and C3 phases, i.e. the following peritectic reaction:

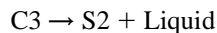
$$\text{C2} \rightarrow \text{C1} + \text{C3}$$

So, apart from the well known C1 (3EO/1Li) compound and the newly observed C3 compound we have detected a third molecular adduct of PEO and LiTf. Table 2 gives the stoichiometry of the different compounds as well as their transition temperature and characteristic X-ray peak position.

The next transition (168°C) is a simple eutectic reaction. Again, the intersection of the two linear segments describing Δh (168°C) vs. X_s (Fig. 4(b)) is located at the eutectic stoichiometry ($X_{s,\text{eutectic}} \approx 0.40$).

On the high salt concentration side of the diagram (i.e. $X_s > 0.60$) the invariant reaction observed at 179°C can be attributed to the pure salt phase transition from a monoclinic to an orthorhombic lattice. As this transition is observed only for $X_s > 0.60$ (see Fig. 4(a)), the pure salt is present only for salt contents higher than that of the C3 compound.

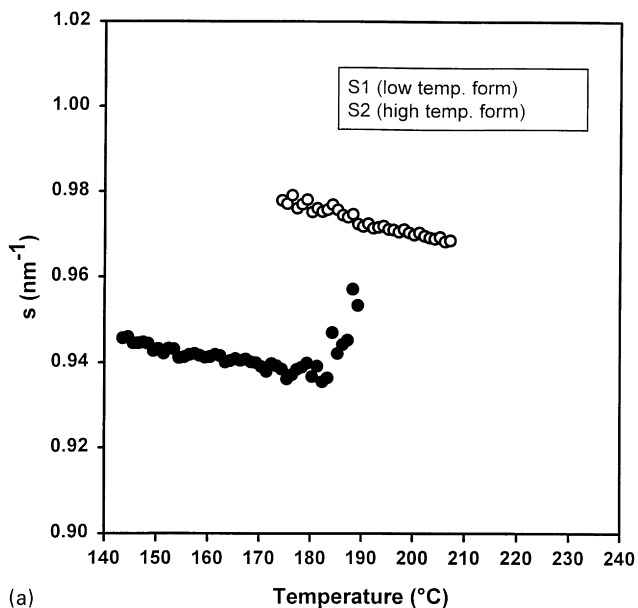
The 198°C transition is also a reaction involving a three phase equilibrium. Fig. 4(c) which gives the Δh vs. X_s evolution for this transition indicates that these phases are the C3 compound ($X_s = 0.60$), pure salt ($X_s = 1$) and a third phase with $X_s = 0.38$ respectively. X-ray data obtained for a sample with $X_s = 0.515$ confirm that the C3 compound disappears around 200°C while a pure salt (S2) crystalline phase develops (Fig. 9). The middle curve in Fig. 11 illustrates the shift of the C3 reflection from 0.985 nm^{-1} to 0.978 nm^{-1} which is characteristic of the pure salt at c.a. 200°C . The diffraction pattern above 200°C is that of pure salt proving that the third phase involved in this reaction is not crystalline. Optical microscopy further confirmed that a large fraction of the sample was then in the liquid state. This interpretation of the 198°C reaction in terms of a peritectic decomposition of C3:



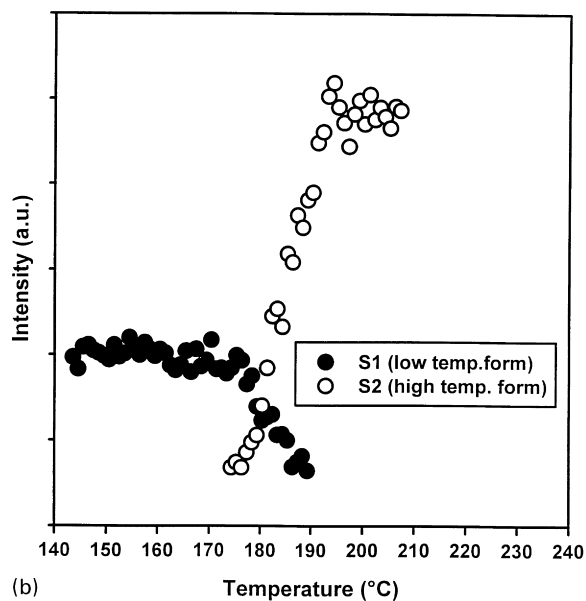
is further validated by the analysis of the diffraction behaviour of the sample with $X_s = 0.654$ (Figs. 10 and 11 lower curve). The almost pure C3 compound is first observed.

Table 1
Indexation of the WAXD pattern for the high temperature form of LiTf

h	k	l	d_{calc} (nm)	d_{obs} (nm)	$(d_{\text{obs}} - d_{\text{calc}})/d_{\text{obs}}$ (%)
1	0	1	1.032	1.032	0.00
0	2	2	0.512	0.514	0.32
1	3	1	0.444	0.444	0.00
4	1	0	0.363	0.364	0.38
4	2	0	0.334	0.334	0.00
0	2	4	0.321	0.321	0.00
3	1	4	0.285	0.284	-0.09
4	1	4	0.254	0.254	0.00



(a)



(b)

Fig. 6. Position (a) and intensity (b) of the first LiTf reflection as a function of temperature.

Below 180°C, the 0.985 nm⁻¹ peak can thus be attributed to a C3 reflection (Fig. 11), the peak then shifts to the pure salt (high temperature S2 form) position. An intensity maximum is then observed (Fig. 10). This intensity maximum is simply the result of the transformation of pure LiTf into the S2 form (for which the diffracted intensity around 1 nm⁻¹ is larger than that of the S1 form as illustrated in Fig. 6(b)) followed by the decrease of the C3 peak located almost at the same position. Once the C3 compound as completely disappeared because of the peritectic reaction, the intensity further increases as a result of crystallization of pure salt.

The last transition at 218°C is more difficult to interpret.

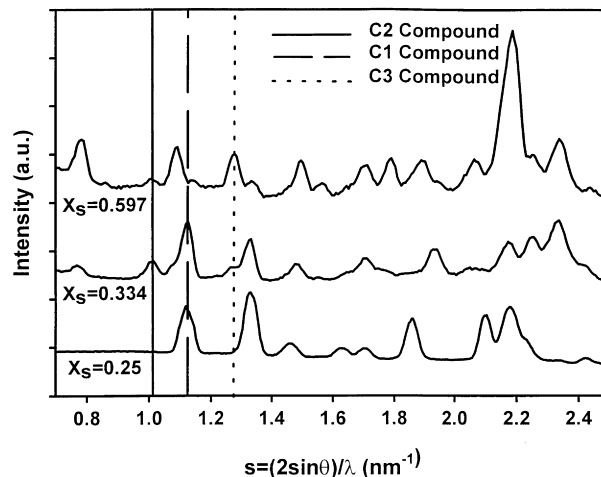


Fig. 7. X-ray diffraction pattern of PEO/LiTf samples with different compositions, the characteristic reflections of each of the observed compound are labelled.

The evolution of Δh (218°C) vs. X_s displays a maximum around $X_s = 0.45$ (Fig. 4(d)) and indicates that this transition, which is very faint at concentrations above $X_s = 0.60$, vanishes for the pure salt. From this behaviour and the general shape of the phase diagram we suggest that for $0.36 < X_s < 0.63$ a liquid–liquid phase separation occurs and that, for $X_s > 0.63$ the pure LiTf dissolves in liquid PEO.

The stoichiometries of the crystalline compounds between PEO and LiTf that were detected in this phase diagram are thus 3EO/1Li (compound C1), 2EO/3Li (compound C2) and 3EO/2Li (compound C3) respectively.

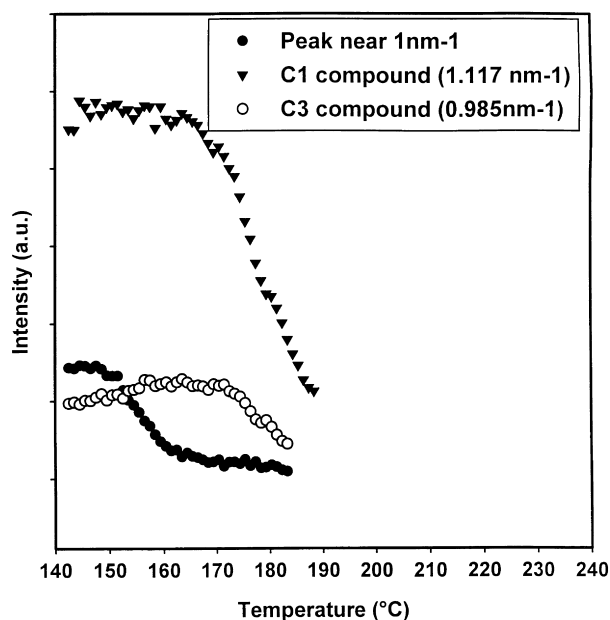


Fig. 8. Diffracted Intensity for the $X_s = 0.334$ sample.

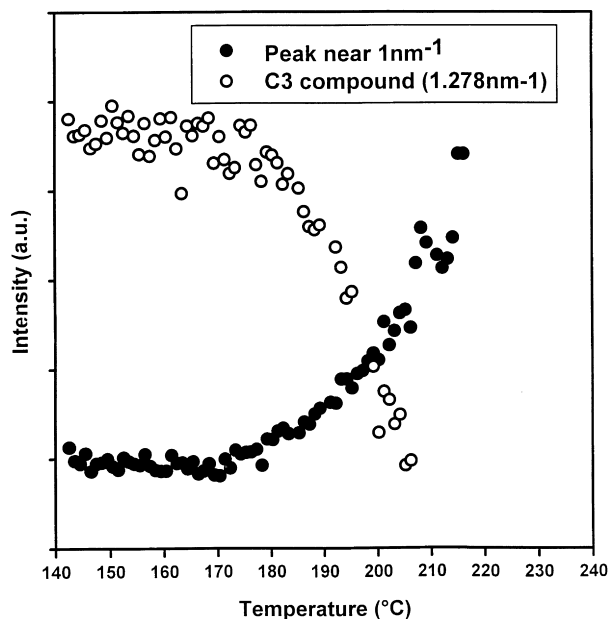


Fig. 9. Diffracted Intensity for the $X_s = 0.515$ sample.

5. Conclusions

High temperature polymorphism of the pure lithium trifluoromethane sulfonate involving a transition from monoclinic to orthorhombic phase at 179°C has been reported for the first time.

The study of the PEO/LiTf system has firstly demonstrated the dramatic effect of sample preparation upon morphology, and properties of the polymer electrolytes. Different procedures can lead to radically different phase diagrams reflecting the existence of a range of metastable

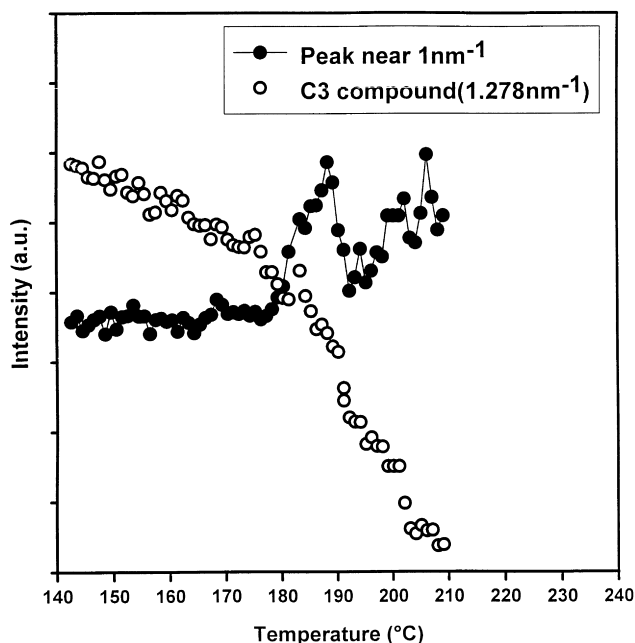


Fig. 10. Diffracted Intensity for the $X_s = 0.654$ sample.

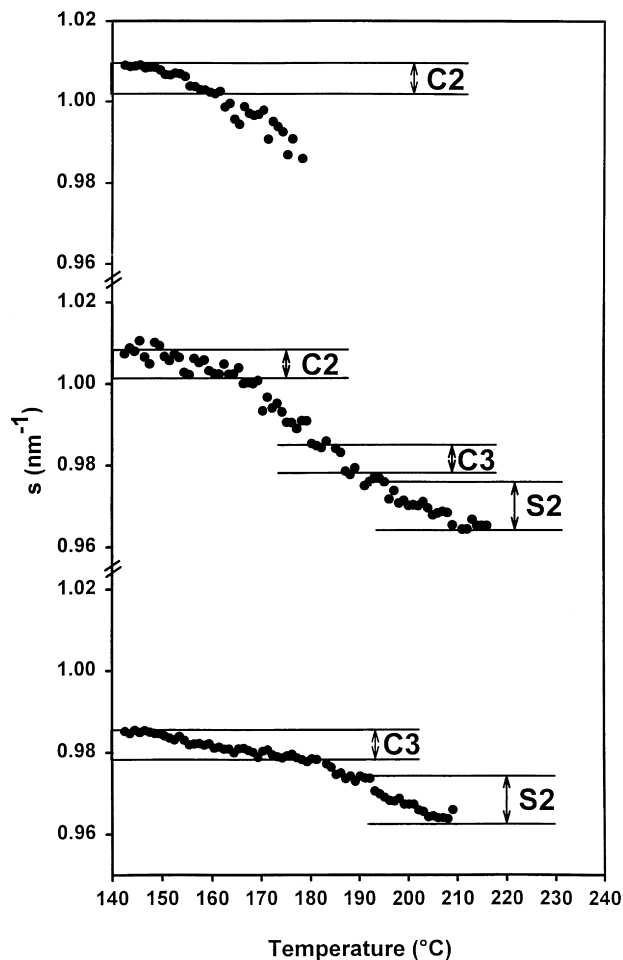


Fig. 11. Exact position of the diffraction peak near 1 nm^{-1} for three samples with $X_s = 0.334$ (upper curve), $X_s = 0.515$ (middle curve) and $X_s = 0.654$ (bottom curve).

states. Three different molecular compounds were observed in the present study: the well characterized 3EO/1Li compound and two other forms with 2EO/3Li and 3EO/2Li stoichiometries respectively. The annealing procedure leads to the formation of these phases from other metastable states that could involve other molecular adducts.

The existence of, at least, three different molecular compounds between PEO and LiTf opens new perspective regarding the study of the complexation effect on chain conformation. Clearly, more detailed crystallographic investigations of these systems are required and the phase diagram obtained here provides a good starting point.

Acknowledgements

This work was supported by Belgian National Fund For Scientific Research (F.N.R.S.) and the European Community Science Program for the access to the D43 beamline at the synchrotron radiation facility at L.U.R.E. (Centre Universitaire de Paris-Sud, Orsay, France). Dr J. Doucet is gratefully acknowledged for his help during the X-ray diffraction

Table 2
Characteristic data for each compound

Compound	Stoichiometry (X_s , EO/Li)	Transition temperature	Position of the characteristic X-ray reflection (s, nm^{-1})
Pure LiTf low temp. Form (S1)		179°C	0.980 (at room temp.) 0.946 (at 140°C)
Pure LiTf high temp. Form (S2)		Degradation before melting c.a. 430°C [7]	0.978 (at 200°C)
C1	$X_s = 0.25$ 3EO/1Li	Congruent melting 174°C	1.117 (at 140°C)
C2	$X_s = 0.60$ 2EO/3Li	Peritectic decomposition 156°C	1.010 (at 140°C)
C3	$X_s = 0.40$ 3EO/2Li	Peritectic decomposition 198°C	1.278 and 0.985 (at 140°C)

experiments at the LURE synchrotron facility in Orsay (France). Dr. M Koch is gratefully acknowledged for fruitful discussion. P. Damman is a Research Associate of the Belgian National Fund For Scientific Research (F.N.R.S.).

References

- [1] Armand MB, Chabagno, JM, Duclot M. Second International Meeting on Solid Electrolytes, St Andrews, Scotland, 20–22 Sept., 1978, Extended Abstract.
- [2] Chatani Y, Okamura S. *Polymer* 1987;28:1815.
- [3] Chatani Y, Fujii Y, Takayanagi T, Honma A. *Polymer* 1990;31:2238.
- [4] Lightfoot P, Mehta MA, Bruce PG. *Science* 1993;262:883.
- [5] Paternostre L, Damman P, Dosière M. *Macromolecules*, in press.
- [6] Robitaille CD, Fauteux D. *J Electrochem Soc* 1986;133:315.
- [7] Vallée A, Besner S, Prud'Homme J. *J Electrochim Acta* 1992; 37:1579.
- [8] Moulin J-F, Damman P, Dosière M. *Macromol Symp* 1997;114: 237.
- [9] Vallée A, Besner S, Prud'Homme J. *Macromolecules* 1989;22:3029.
- [10] Tremayne M, Lightfoot P, Mehta MA, Bruce PG, Harris KDM, Shankland K, Gilmore CJ, Bricogne G. *J Solid State Chem* 1992; 100:191.
- [11] Banka PA, Selser JC, Wang B, Shenoy DK, Martin R. *Macromolecules* 1996;29:3956.